Ocean Systems Engineering, *Vol. 15, No. 3 (2025) 327-344*
https://doi.org/10.12989/ose.2025.15.3.327

Investigation of high order hydrodynamic load influence on a TLP FOWT

Chunhui Song[1], Shenglei Fu[1], Yuming Zhang[1], Yunlong Su[1], Alex Ran[2], Jim Li[2] and Tuanjie Liu[*2]

[1]*CNOOC, LTD, China*
[2]*OffshoreTech China, LLC, China*

(Received May 27, 2025, Revised September 10, 2025, Accepted September 17, 2025)

Abstract. The influence of the second and third order wave loads on the TLP FOWT responses are investigated in this study. The second order wave loads are calculated by commercial wave diffraction/radiation analysis software tool. The third order wave loads calculation methods are developed in this study based on the well-known FNV formulation. The third order wave force is applied on the platform in dynamic simulation models as external force. It is observed that the third order wave force is cubic proportional to the wave heights. The sum frequency third order wave force has periods about 1/3 of the first order wave periods. With the same wave heights, the third order wave forces on the surface piercing structure are higher in shallower waters. The 2nd order wave loads have higher influences on the FOWT responses than the 3rd order wave loads in both fatigue and extreme load cases. The 3rd order wave force influence is negligible in fatigue load cases. The high order wave loads have more impact on the tower and mooring system responses than platform motion. On a TLP FOWT, the tower and mooring system usually feature high frequency resonance susceptible to excitation from sum frequency 2nd and 3rd order wave loads.

Keywords: FNV formulation; high order hydrodynamic load; TLP FOWT

1. Introduction

Offshore wind is considered as one of the fastest-growing sources of clean and renewable energy. While fixed-type offshore wind turbines made significant contributions to total wind energy production, they are limited by water depth, typically less than 50m. On the other hand, Floating Offshore Wind Turbines (FOWTs) offer the ability to capture steadier and stronger wind energy in deeper waters. As one of the four main FOWT concepts, the tension leg platform (TLP) floater has gained more attention in recent years in the offshore wind industry. TLPs feature low floater motions and substantially reduced mooring footprint compared to other concepts like semi-submersibles and Spars (Bachynski and Moan 2012). In contrast to other floater types with spread mooring systems, the stability of TLPs is provided by tensioned vertical or near vertical mooring lines (tendons). However, this design results in high mooring stiffness and natural frequency in the vertical degree of freedom. Consequently, TLP FOWTs are subject to resonant

*Corresponding author, Ph.D., E-mail: tuanjie.liu@offshoretechllc.com

 ISSN: 2093-6702 (Print), 2093-677X (Online)

Fig. 1 A 16 MW TLP FOWT Concept

responses such as “ringing” and “springing” to high order wave loads in the mooring lines (Bachynski and Moan 2014). Therefore, it is necessary to investigate the second and third order wave effects on TLP FOWTs.

Bae and Kim (2011a, b) investigated a 1.5 MW TLP FOWT with fully coupled dynamic analysis in time domain including aero-blade-tower dynamics and control, mooring dynamics, and platform motions. The results were compared against uncoupled cases and concluded that the system dynamic responses increased in the fully coupled analysis. In addition, the platform pitch natural frequency shift due to the flexibility of the tower was observed. This indicates that duly considering the flexibility of the tower and its coupling effect with the floater are very important to accurately predict the high frequency responses of the TLP FOWT in the vertical plane.

Ringing of conventional TLPs may occur in steep wave conditions (Faltinsen *et al.* 1995). The hydrodynamic loading driving such responses have been widely studied (Bachynski and Moan 2014, Faltinsen *et al*. 1995, Tromans *et al*. 2016). TLP FOWTs, particularly single column designs with relatively large diameters, are susceptible to high order wave load effects. Bae and Kim (2013) examined the effect of second-order wave force on the mono-column TLP-type FOWT. It was observed that the second-order sum-frequency wave loading introduced high-frequency excitations near pitch-roll resonance frequencies or lowest tower flexural modes. The increased high-frequency responses may significantly increase tower top accelerations and tower base reaction forces.

Most of the current software tools for FOWT design and analysis based on nonlinear frequency domain potential flow method are able to include second order wave forces. In order to calculate the third order wave forces, a non-linear wave force model for cylindrical structures is required. Newman (1996) developed formulation for third order horizontal wave force on a vertical cylinder in random waves based on Faltinsen, Newman, Vinje (FNV) formulation (Faltinsen *et al*. 1995).

Table 1 Principal Dimensions of the 16 MW TLP FOWT

Principal Dimensions		Unit	Value
Center column	Diameter	m	14.0
	Length	m	36.0
Pontoon	Length	m	43.0
	Width	m	6.0
	Height	m	7.0
Distance between pontoon ends		m	86.6
Distance from column center to pontoon ends		m	50.0
Tower	Length	m	127.6
	Base diameter	m	10.0
	Top diameter	m	5.95
	Mass (with RNA)	t	1700
Operating draft		m	23.0
Displacement at operating draft		t	~11075

Malenica and Molin (2006) developed a method to solve the third-order problem based on eigenfunction expansions and on the integral equation technique with the classical Green function expressed in cylindrical coordinates. Teng and Dong (2001) developed a numerical method for the third-order triple-frequency wave loads on fixed axisymmetric bodies in monochromatic incident waves.

In this paper, the method of high order wave load calculation for a typical single column TLP type FOWT based on FNV (Faltinsen 1995, Newman 1996) formulation is utilized on a 16 MW TLP FOWT concept design as shown in Fig. 1. Key responses including platform motion, tower base reaction force, and mooring line tension will be compared to evaluate the influence of the second and third order wave forces.

The viscous effects of slender members such as the pontoons, center column, and braces are computed by Morison's formula and are combined with the potential forces to compute the wave forces on the platform. Morison nonlinear viscous drag may contribute to the 3rd harmonic force on the platform. However, this paper only considers potential-flow forces and high-order contributions from viscous forces are not investigated.

2. TLP FOWT platform description

The TLP FOWT is a single column configuration with three rectangular cross-section pontoons radially arranged near the bottom of the center column. The column diameter is 14 m and the in-place draft of the platform is 23 m. The total displacement of FOWT is about 11,075 MT. The platform is designed for an anonymous field with 140 m water depth. The FOWT will be moored by a wire rope mooring system composed of three (3) bundles. Each bundle comprises of two (2) mooring lines. The mooring lines are inclined with a 10.9 degrees angle. The design mooring pretension is 500 MT. Table 1 summarizes the principal dimensions of the platform. Table 2 presents the mooring line properties

Table 2 Mooring Line Properties

Line type	Parameters	Unit	Value
Wire rope	Diameter	mm	153
	Length	m	118.88
	Weight in Air(in Water)	Kg/m	123(99.1)
	Stiffness (EA)	MN	2146
	MBL	kN	25302

Table 3 TLP FOWT Natural Periods

Surge	Sway	Heave	Roll	Pitch	Yaw	Tower (1st flap wise)
41.05	41.05	1.60	0.91	0.91	18.60	4.22

Mode analysis is carried out in OrcaFlex for the TLP FOWT with mooring system. The results are listed in Table 3. The pontoon and column are modeled as rigid bodies, The rotor-nacelle-assembly (RNA) is modeled with a 6x6 mass matrix without blade flexibility. Therefore, natural period of the blades is not calculated.

The TLP FOWT hull surface is modeled using quadrilateral and triangular panels and analyzed using 3-D panel method with diffraction theory (including first- and second- order wave loads). The diffraction force, added mass, and radiation damping on the hull are obtained and then imported by OrcaFlex for dynamic simulations.

3. Calculation of high order hydrodynamic loads

3.1 Calculation of the second order wave loads

The second-order wave loads acting on an offshore structure include mean, difference-frequency, and sum-frequency components. These are of special importance to platforms with low- or high-frequency resonant features outside the spectral range of wave encountered. Numerical methods are used for evaluating the second-order loads, based on extensions of the first-order panel method and applicable to three-dimensional structures of arbitrary geometric form.

The second order wave forces on the TLP FOWT in this study are calculated by hydrostatic/hydrodynamic analysis tool SESAM/WADAM. Fig. 2 shows panel model for the platform first- and second order wave force calculations. For the second-order diffraction problem, additional free-surface panels up to the truncation radius are needed. Figs. 3 and 4 show the difference- and sum-frequency full QTFs for surge, heave, and pitch DOFs. It can be observed from the difference-frequency full QTFs that the diagonal values (mean drift loads) are generally lower than off-diagonal values. In addition, the sum-frequency QTF values are the same order of magnitude with the difference-frequency QTFs. These observations indicate that including both difference- and sum-frequency full QTFs in TLP FOWT numerical simulation is necessary to obtain accurate dynamic response results.

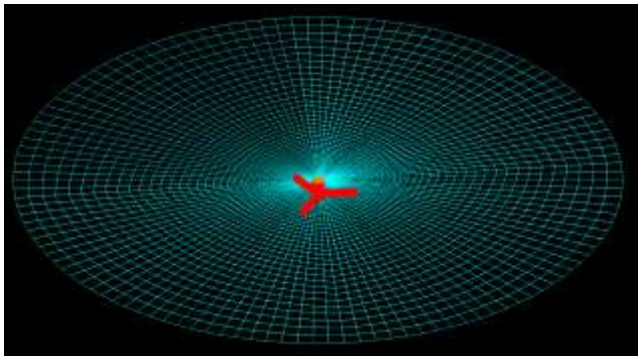

Fig. 2 Hydrodynamic Panel Model for the TLP FOWT

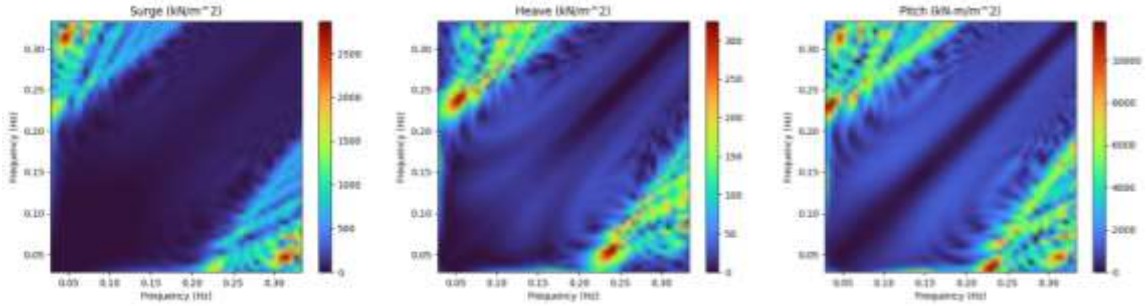

Fig. 3 Difference-frequency Full QTFs

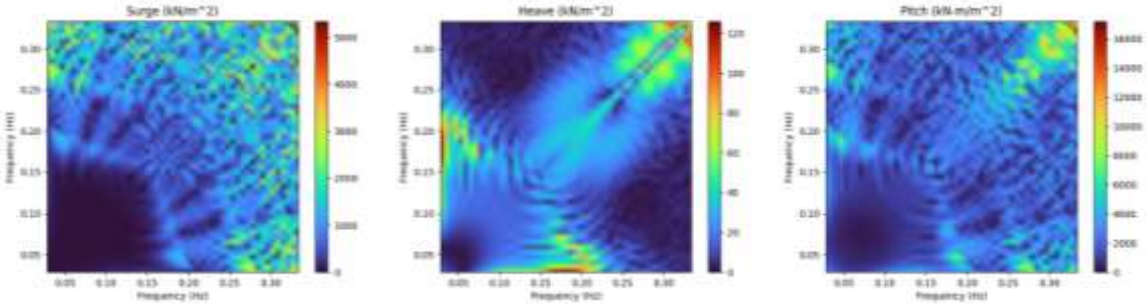

Fig. 4 Sum-frequency Full QTFs

4. Calculation of the third order wave loads

The third order wave forces on simple structures like a vertical cylinder can be evaluated with analytical methods. The current TLP FOWT features a single column at the center of the platform. Therefore, in order to evaluate the third order wave loads, the platform can be approximated as a single cylinder extending from the column deck to the platform keel.

The well-known Faltinsen, Newman, Vinje (FNV) long-wave formulation (Faltinsen *et al*. 1995) for the horizontal forces on a vertical cylinder due to the third order potential was extended to irregular waves by Newman (1996). While the second order component of the long-wave excitation force has been shown to compare well to full second-order diffraction only up to approximately ka = 0.1, the third order FNV formulation is known to compare well to full third order diffraction theory up to ka = 0.4 (Krokstad *et al*. 1998).

The direct implementation of Newman's irregular wave formulation (Newman 1996) is adopted in this study for the third order hydrodynamic load estimation for the TLP FOWT.

For an infinitely deep, surface-piercing vertical circular cylinder, the third order force $F_3^{(1)}$ due to the first order potential is given by Newman (1996):

$$F_3^{(1)} = \pi\rho a^2 \left[\zeta_1 \left(u_{tz}\zeta_1 + 2ww_x + uu_x - \frac{2}{g}u_t w_t\right) - (u_t/g)(u^2 + w^2)\right] \tag{1}$$

where ρ is the water density, g is the acceleration due to gravity, ζ_1 is the first order wave elevation, a is the radius of the cylinder, and u and w are the horizontal and vertical wave particle velocity, respectively. Differentiation is indicated by subscripts. The third order force due to the nonlinear (second order) potential is given as

$$F_3^{(2)} = a\int_0^{(h+\zeta_1)/a} (\pi\rho a/g)u^2 u_t(3\Psi_1 + 4\Psi_2)\, dZ \tag{2}$$

Where $Z = (\zeta_1 - z)/a$, and h is the cylinder draft. The definitions of the nondimensional functions $\Psi_1(Z)$ and $\Psi_2(Z)$ (spatially-varying components of the solution to Laplace's equation for a stationary vertical cylinder) can be found in (Faltinsen *et al*. 1995, Newman 1996) and expressed as follows.

$$\Psi_m(1, Z) = -\frac{2}{\pi}\int_0^\infty F_m(k)e^{-kZ}\frac{k^{-1}dk}{J\prime_m(k)^2 + Y\prime_m(k)^2} \tag{3}$$

$J'_m(k)$ and $Y'_m(k)$ are derivatives of Bessel functions of the first and the second kinds, respectively. The definitions of $F_m(k)$ can be found in (Faltinsen *et al.* 1995).

For $m = 1$

$$\Psi_1(1, Z) = -\frac{2}{\pi}\int_0^\infty F_1(k)e^{-kZ}\frac{k^{-1}dk}{J\prime_1(k)^2 + Y\prime_1(k)^2} \tag{4}$$

$$\mathrm{F}_1(k) = -\frac{2}{\pi k}\left[\frac{13}{12} - \frac{7}{32}k^2 - \frac{1}{192}k^4 + \left(\frac{1}{4}k^3 + \frac{1}{192}k^5\right)\left(kS_{-1,0} + S'_{-1,0}\right)\right] \tag{5}$$

Here the prime sign indicates differentiation of the Lommel function $S_{-1,0}$ with respect to the argument k. The following expression can be used to compute Eq. (5).

$$kS_{-1,0} + S'_{-1,0} = -\frac{\pi k}{2}\left[Y'_1(k)\int_k^\infty J_0(x)x^{-1}dx - J'_1(k)\int_k^\infty Y_0(x)x^{-1}dx\right] \tag{6}$$

The following methods for evaluating the integrals in Eq. (6) are described in Abramowitz and Stegun (1964, Chap. ll), and by Luke (1969).

$$\int_k^\infty \frac{J_0(x)}{x}dx = -\gamma - \ln\frac{k}{2} - \sum_{m=1}^\infty \frac{(-1)^m\left(\frac{k}{2}\right)^{2m}}{2m(m!)^2} \tag{7}$$

Where $\gamma = 0.57721566490153286$, is the Euler-Mascheroni constant.

$$\int_k^\infty \frac{Y_0(x)}{x}dx = -\frac{1}{\pi}\left(\ln\frac{k}{2}\right)^2 - \frac{2\gamma}{\pi}\ln\frac{k}{2} + \frac{1}{\pi}\left(\frac{\pi^2}{6} - \gamma^2\right) + \frac{2}{\pi}\sum_{m=1}^\infty \frac{(-1)^m\left(\frac{k}{2}\right)^{2m}}{2m(m!)^2}\left[\psi(m+1) + \frac{1}{2m} - \ln\frac{k}{2}\right] \quad (8)$$

The Psi function (or Digamma function) $\psi(z)$ is defined as

$$\psi(z) = \frac{d[\ln\Gamma(z)]}{dz} = \Gamma'(z)/\Gamma(z) \quad (9)$$

The above method is valid for small k values, and diverges at $k = 23.5$.

For large k values, $F_1(k)$ can be evaluated using the following asymptotic expansion.

$$F_1(k) \sim -\frac{12}{\pi k^3}\left[1 - \frac{1}{36}\sum_{m=1}^\infty \left(-\frac{4}{k^2}\right)^m (m+1)!\,(m+2)!\,(2m^3 + 17m^2 + 23m - 18)\right] \quad (10)$$

The above expression has 9% error for $k = 16$, 3.6% error for $k = 17$, 1.6% error for $k = 18$, 0.7% error for $k = 19$, and 0.3% error for $k = 20$.

Eqs. (5) to (9) present a method for evaluation of $F_1(k)$ for small k values, and Eq. (10) is a complementary formulation for large k values. It is recommended that the former is applied for $k \leq 20.0$, and the latter is applied for $k > 20.0$.

For $m = 2$

$$\Psi_2(1, Z) = -\frac{2}{\pi}\int_0^\infty F_2(k)e^{-kZ}\frac{k^{-1}dk}{J'_2(k)^2 + Y'_2(k)^2} \quad (11)$$

And the function $F_2(k)$ takes a much simpler form as follows

$$F_2(k) = -\frac{8}{\pi k^3} \quad (12)$$

Therefore, Eq. (11) can be rewritten as

$$\Psi_2(1, Z) = \frac{16}{\pi^2}\int_0^\infty e^{-kZ}\frac{k^{-4}dk}{J'_2(k)^2 + Y'_2(k)^2} \quad (13)$$

At this point, Eqs. (4) and (13) can be evaluated using numerical integration method. The purpose of deriving $\Psi_1(1, Z)$ and $\Psi_2(1, Z)$ is to calculate the third order force due to the nonlinear (second order) potential which is given in Eq. (3). which can be evaluated numerically.

The calculated third order wave load is to be applied as horizontal point force with the action point near the mean water level. In OrcaFlex dynamic analysis models, the force can be introduced as variable external load force on the floating platform.

5. Validation of the third order wave loads calculation

According to the derivations of the functions Ψ_1 and Ψ_2, the calculation procedures are very complicated. Direct integration of special functions with singular points needs to be avoided if possible. Therefore, converting integrals into series as described above is necessary. Fig. 5 illustrates the validation of functions Ψ_1 and Ψ_2 calculations. The plot on the left-hand side is from (Faltinsen *et al*. 1995) and the plot on the right-hand side is generated from the calculation methods presented in this study. It can be observed that plots from both studies have perfect match.

A simple time-series simulation is presented in (Newman 1996) to illustrate the results of the above analysis method. To conform with the characteristic wave amplitude and frequencies of extreme waves, the first-order free-surface elevation is constructed from five sinusoidal

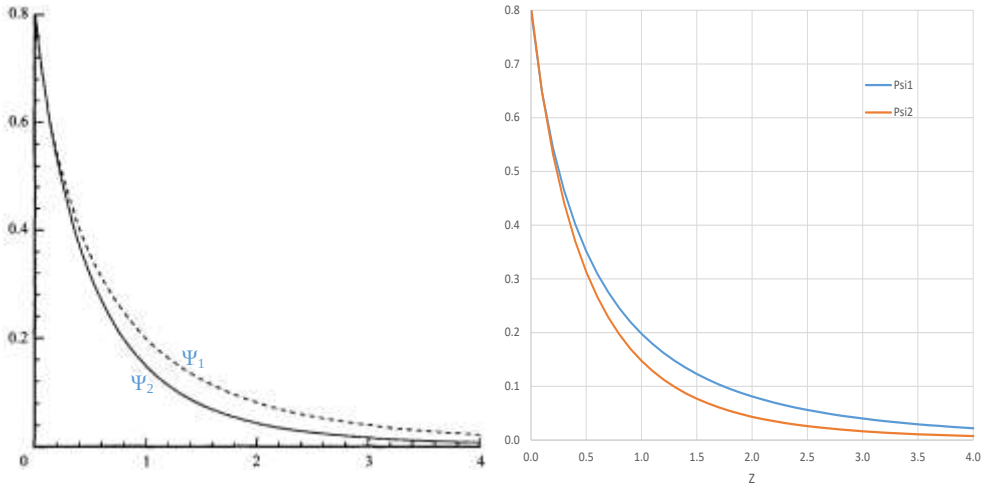

Fig. 5 Validation of Functions Ψ1 and Ψ2 Evaluation

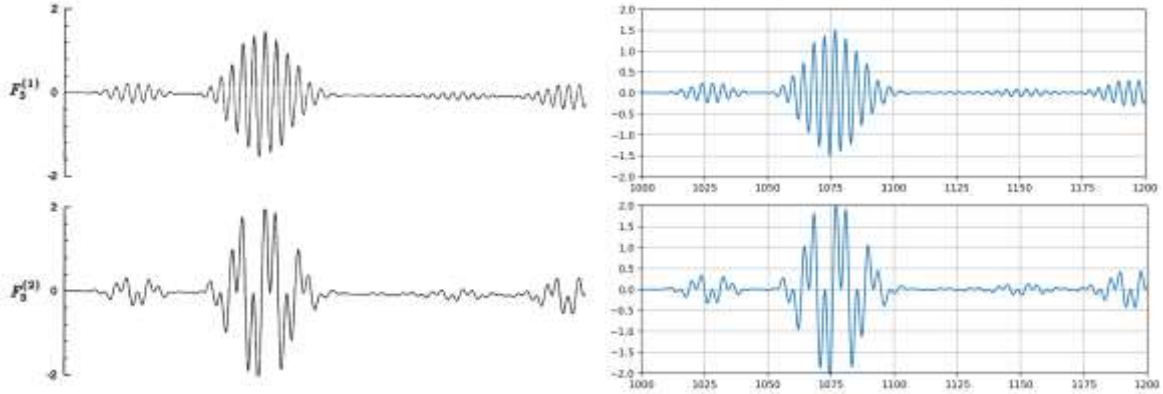

Fig. 6 Validation of the Third Order Wave Force Calculation

components in the form

$$\zeta_1 = \sum_{n=1}^{5} A_n \sin \omega_n t \tag{14}$$

Where $A_n = 2$ m, $\omega_n = 2\pi/T_n$, and the periods of the five components are $T_n = (11, 12, 13, 14, 15)$ seconds. This includes one 'extreme event' around $t = 1075$ seconds, when the five separate components are nearly in phase and the amplitude approaches ten meters.

Fig. 6 shows the comparison of the third order wave force results between those presented in (Newman 1996) on the left and derivations in this study on the right. The comparison shows that the two sets of calculation results are identical. Note the data curves shown in Fig. 6 are normalized with $\rho g a^2$ and therefore, the data values have a unit of length.

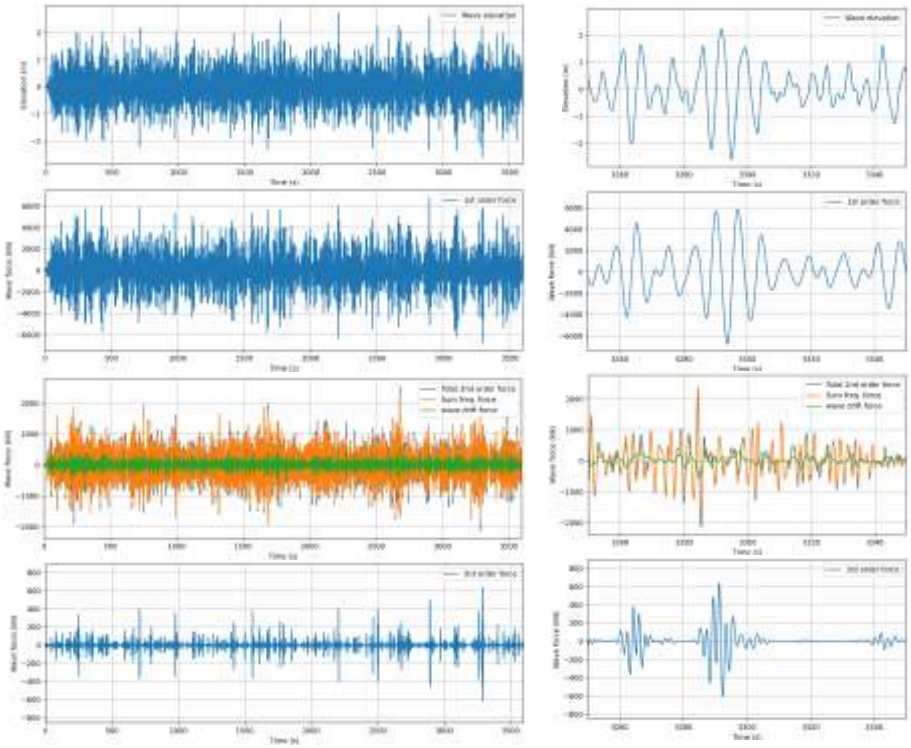

Fig. 6 Validation of the Third Order Wave Force Calculation

Table 4 Load Case Definitions

Load case	H_S [m]	T_P [s]	γ [-]
Fatigue	2.73	8.32	1.2
Extreme	12.7	14.7	2.4

6. High order wave force calculation results

6.1 Load case description

Two typical load cases as listed in Table 4 are selected for the second and third order hydrodynamic load influence on the TLP FOWT: one for fatigue sea state and the other for extreme sea state. In order to eliminate influences from varying wind forces, wind is not considered in the study.

6.2 Wave force comparison

Before investigating the influence of high order hydrodynamic loads on the TLP FOWP, it is necessary to investigate the contributions of the total wave loads from the first, second, and third order components. The first and second order wave forces can be output directly from OrcaFlex

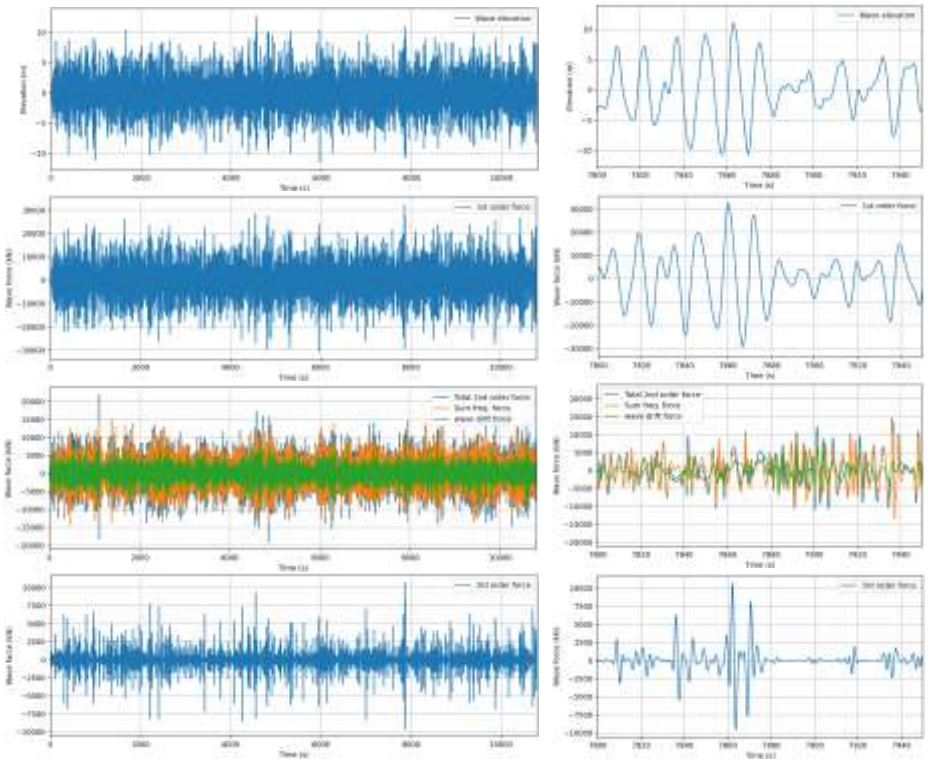

Fig. 8 Wave Force Comparison, Extreme Load Case

simulation models. The third order wave force can be obtained by the calculation method introduced earlier in this paper.

Fig. 7 shows the wave force comparison for the selected fatigue load case with 2.73 m wave height. The four rows of plots from top to bottom are incident wave elevation, the first order wave force, the second order wave force, and the third order wave force. The column on the left includes time histories from 0 to 3600 seconds, and the column on the right includes time histories zoomed in from 3250 and 3350 seconds. The second order wave force plots show wave drift force (difference frequency), sum frequency, and the total second order wave forces. It can be observed from the results that the maximum first order wave force is over 6000 kN, the maximum second order wave force is about 2500 kN, and the maximum third order wave force is over 600 kN. Within the second order wave force components, the sum frequency wave force is the dominant contributor compared to wave drift force. In addition, the third order wave force is more impulsive than the first and second order wave forces. The wave excitations with this feature may cause ringing and springing responses on the TLP type FOWT.

Similarly, wave force comparison for selected extreme load case is shown in Fig. 8. The extreme wave height is 12.7 m. The zoomed in column on the right includes time histories from 7800 to 7950 seconds. It can be observed that the maximum first order wave force is over 30000 kN, the maximum second order wave force is about 21000 kN, and the maximum third order wave force is over 10000 kN. In contrast to the fatigue load case, both the second and third order wave forces have higher proportions in the extreme load case.

7. Platform response results

Dynamic simulations for the two selected load cases defined in Table 1. The time-domain simulation duration is one (1) hour for fatigue load case and three (3) hours for the extreme load case. Within each load case, the following variations are considered to investigate the influence of high order hydrodynamic loads.

- First order wave force only
- First and second order wave forces
- First, second, and third order wave forces

The following critical responses are selected for comparison.

- Platform surge
- Platform heave
- Platform pitch
- Mooring line top tension

Note the wave direction in both fatigue and extreme load cases is 0 degree. Due to symmetry in platform geometry and dynamics, platform sway, roll, and yaw responses are negligible. There are three (3) mooring lines attached to each of the three pontoons. One mooring line from each group is selected for top tension check.

8. FOWT response time histories and power spectral density

8.1 Fatigue load case

Fig. 9 illustrates response time history comparison for the fatigue load case. The first column includes time history plots with time range from 0 to 3600 seconds. The second column includes zoomed in plots for the time range from 2150 to 2250 seconds. According to the comparison, the responses with 1st+2nd+3rd order wave loads are almost identical to those with 1st+2nd order wave loads. The responses in the case with the first order wave force only are marginally different from the other two sets of results.

Fig. 10 shows the power spectral density (PSD) graphs of the selected critical responses in the fatigue load case. According to the PSD comparison, the wave frequency responses are almost identical among the three variation cases. The most noticeable difference exists in the responses near 0.24 Hz which is the tower resonance frequency. The second order wave load excitation causes slightly higher tower resonance in the fatigue load case.

Based on the above comparisons for the fatigue load case, the second order wave load has marginal influence on the platform, tower, and mooring line responses, and the influence from the third order wave force is negligible.

8.2 Extreme load case

Fig. 11 illustrates response time history comparison for the extreme load case. The first column includes time history plots with time range from 0 to 10800 seconds. The second column includes

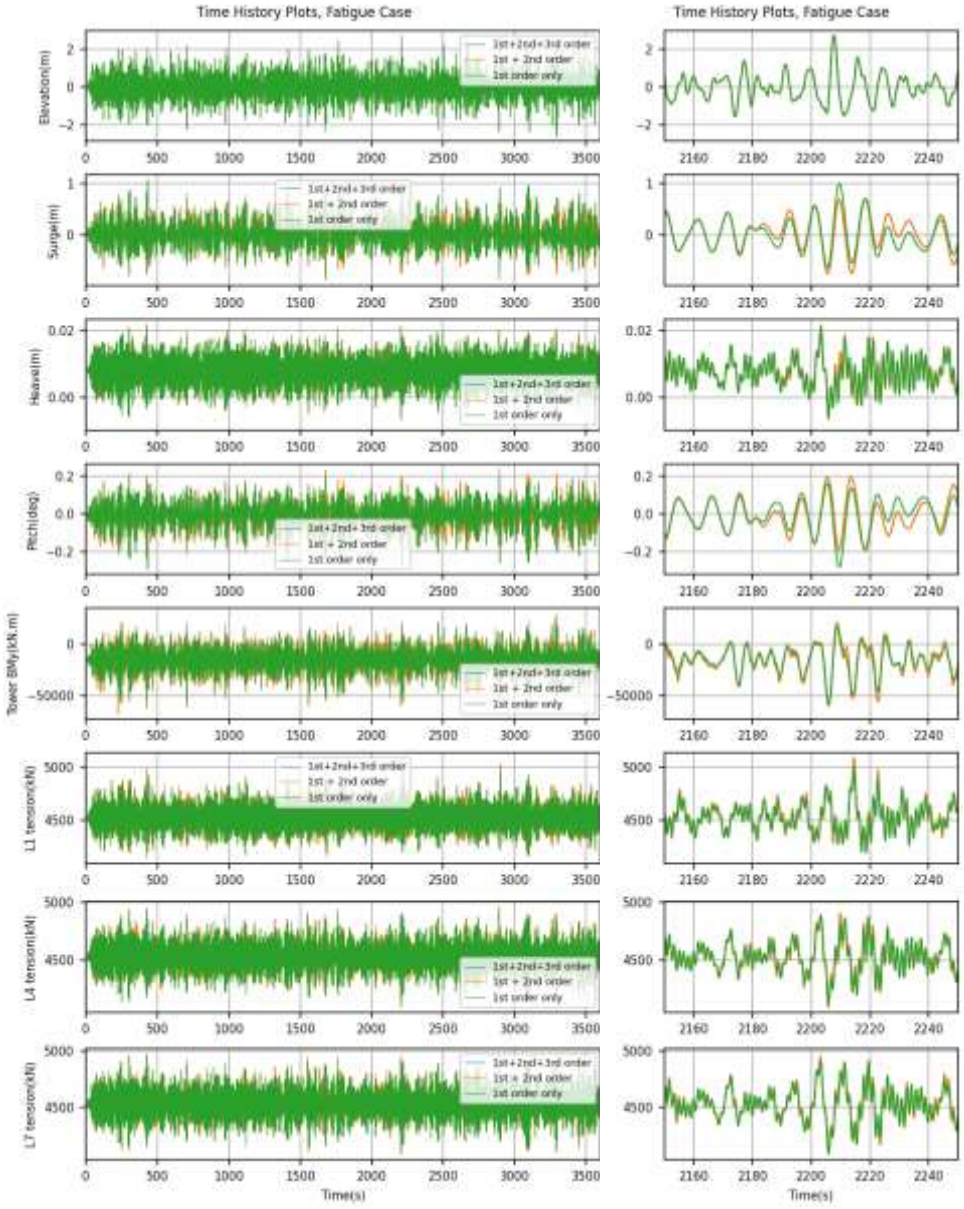

Fig. 9 Platform Response Time History Comparison, Fatigue Case

zoomed in plots for the time range from 5925 to 6025 seconds. According to the comparison, the three sets of time history results are marginally different.

Fig. 12 shows the power spectral density graphs of the selected critical responses in the extreme load case. Similar to the fatigue load case result comparison, the most noticeable difference exists in the responses near 0.24 Hz which is the tower resonance frequency. It should be noted that the tower base bending moment at 0.24 Hz resonance frequency is disproportionally higher than all other responses. This indicates higher order wave forces have significant impact on the tower

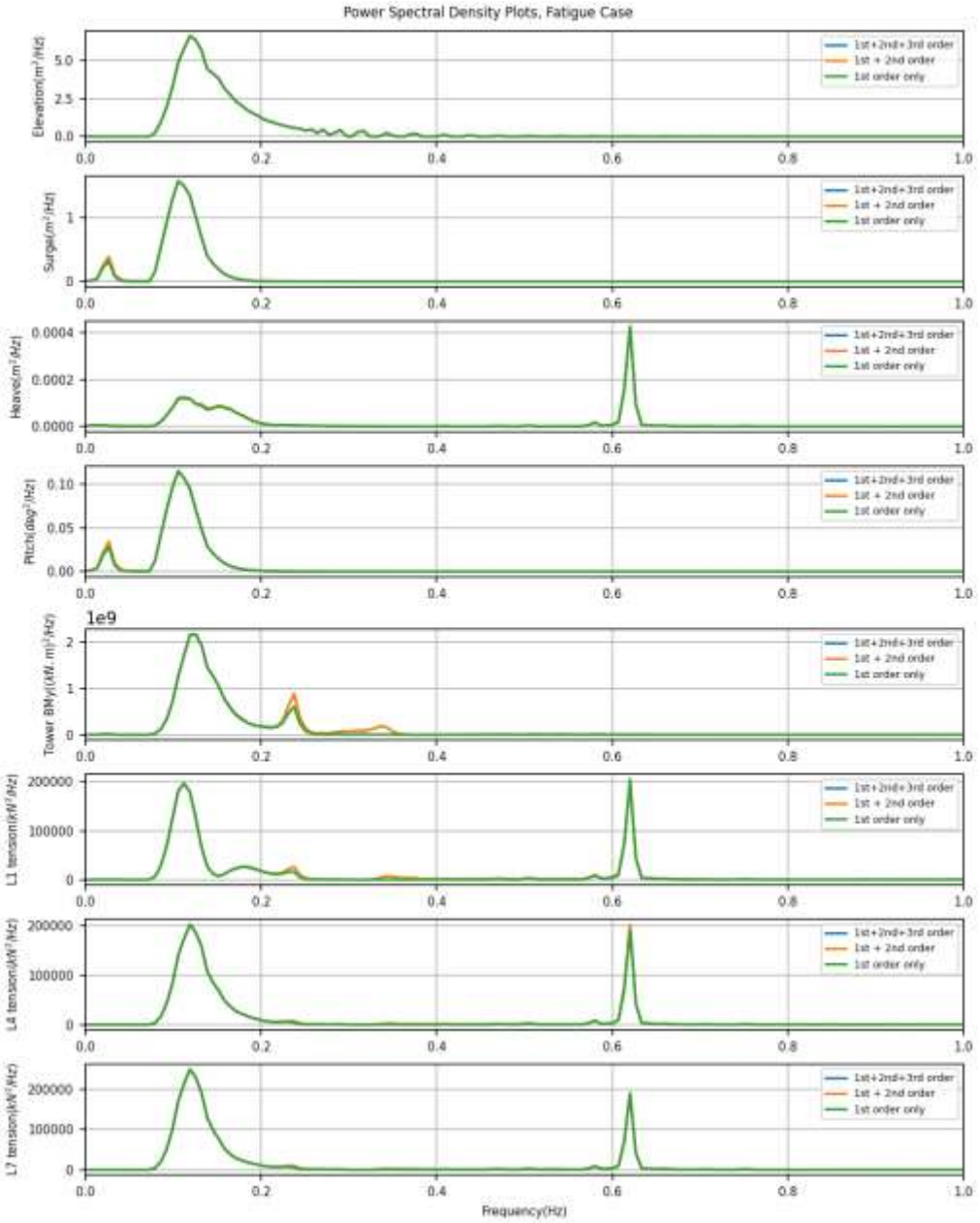

Fig. 10 Platform Response PSD Comparison, Fatigue Case

dynamic responses. In addition, the mooring tension PSD plots show a small hump near 0.62 Hz (heave natural frequency) with 2nd and 3rd order wave loads. However, this hump is not observed in the first order wave load only case. This can be explained that the sum frequency wave loads have excited the mooring system resonance responses. Otherwise, the responses in wave and low frequency range are very close among all three sets of results compared.

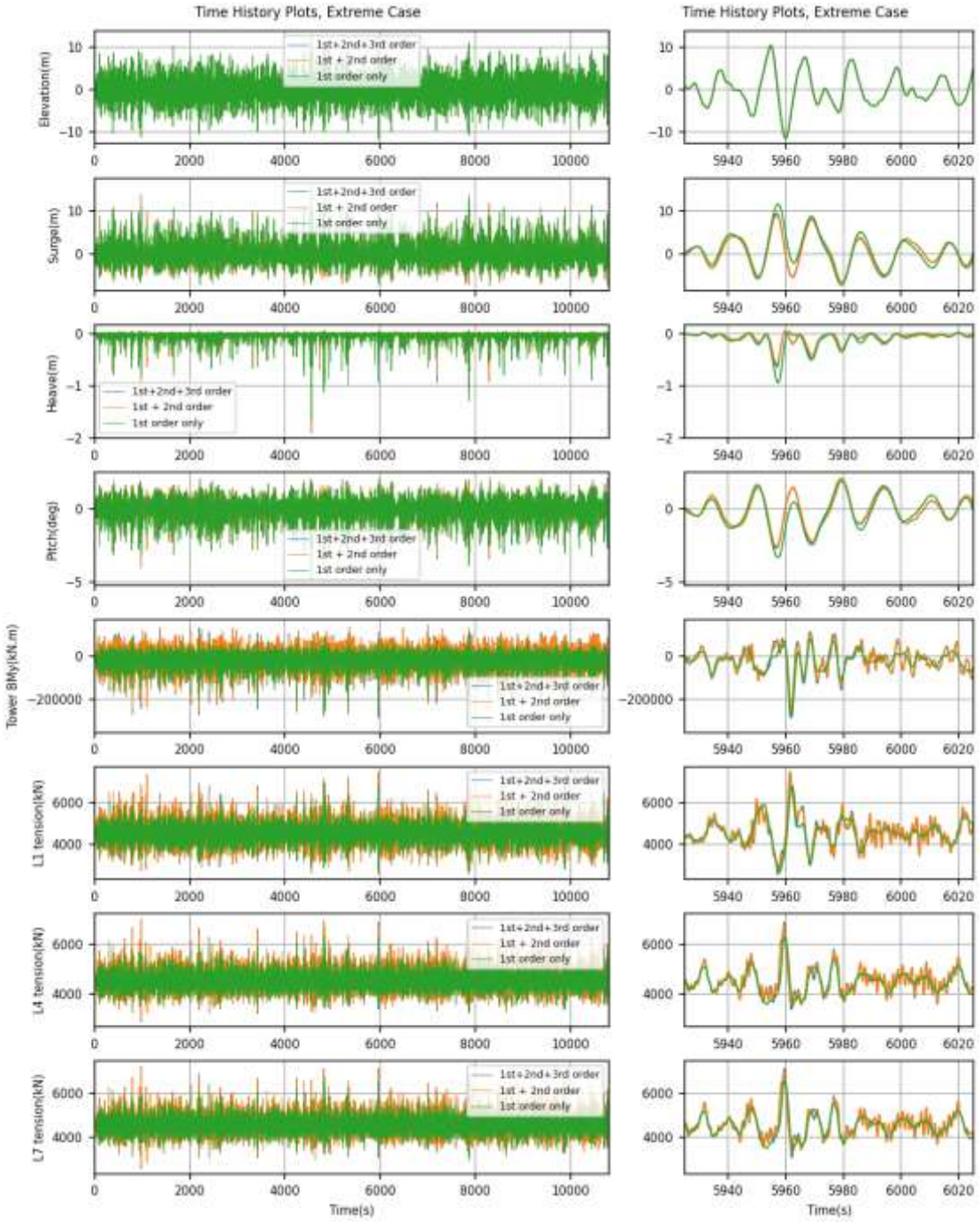

Fig. 11 Platform Response Time History Comparison, Extreme Case

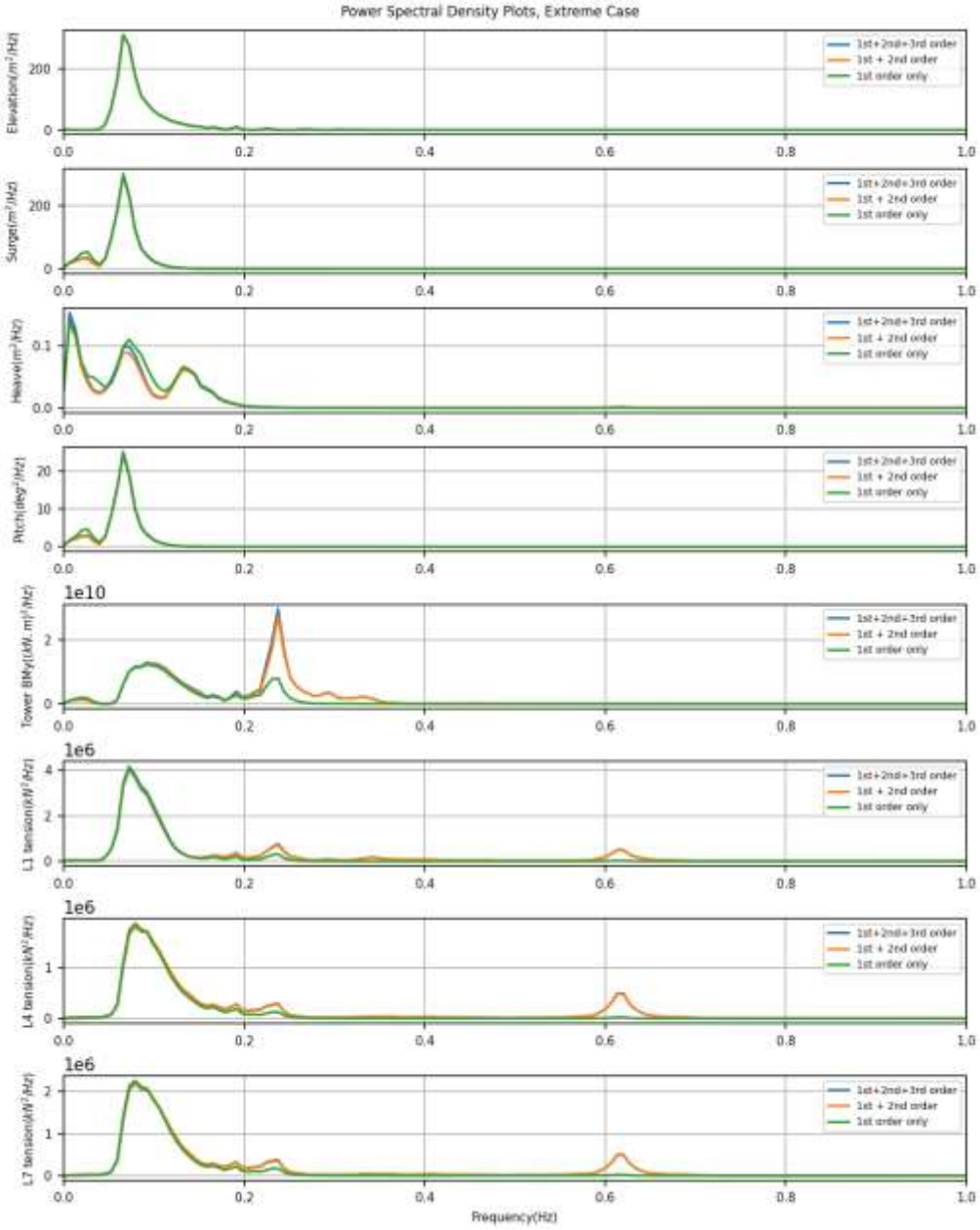

Fig. 12 Platform Response PSD Comparison, Extreme Case

According to the above comparisons for the extreme load case, the second order wave load has considerable influence on the platform, tower, and mooring line responses. The influence from the third order wave force is marginal. Both the 2nd and 3rd order wave loads have larger influences on the FOWT responses in the extreme load case than those in the fatigue load case.

Table 5 FOWT Response Statistics for Fatigue Case

	1st order only			1st + 2nd order			1st+2nd+3rd order		
	Mean	**Max**	**Std**	**Mean**	**Max**	**Std**	**Mean**	**Max**	**Std**
Wave elevation (m)	0.000	2.727	0.684	0.000	2.727	0.684	0.000	2.727	0.684
Surge (m)	0.016	1.067	0.265	0.041	0.905	0.267	0.041	0.912	0.268
Heave (m)	0.008	0.021	0.004	0.008	0.022	0.004	0.008	0.022	0.004
Pitch (deg)	-0.005	0.295	0.072	-0.012	0.242	0.073	-0.012	0.245	0.073
Tower BMy (kN.m)	-15165	62338	11126	-15350	67668	11756	-15350	67633	11804
L1 tension (kN)	4529.0	5006.4	103.6	4529.8	5091.0	107.7	4529.8	5090.5	107.6
L4 tension (kN)	4529.0	4943.9	109.3	4531.4	4958.5	111.9	4531.4	4958.9	111.8
L7 tension (kN)	4527.6	4970.1	117.5	4530.2	4973.4	119.7	4530.2	4974.3	119.5

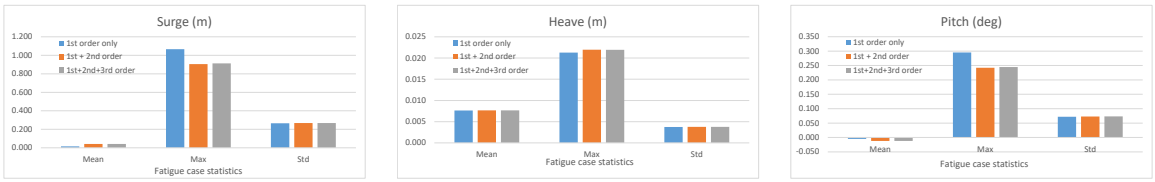

Fig. 13 Platform Surge, Heave, and Pitch Statistics, Fatigue Case

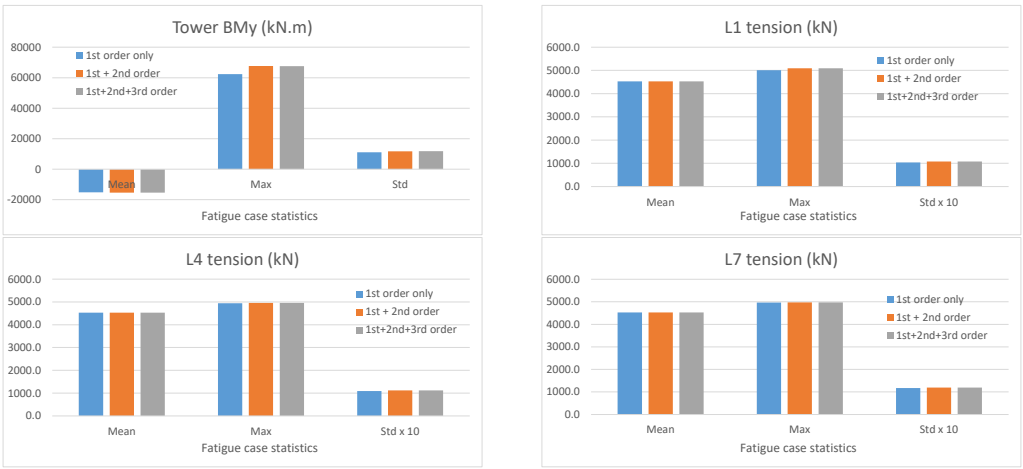

Fig. 14 Tower Base Moment and Line Tension Statistics, Fatigue Case

9. FOWT response statistics comparison

The response statistics, including mean, maximum, and standard deviation. The statistics for the fatigue and extreme load cases are summarized in Tables 5 and 6, respectively. All the comparisons are also illustrated in Fig. 13 to 16.

The statistics show that among three sets of results (three different wave load combinations), (1st+2nd) and (1s +2nd+3rd) are much closer than those first order wave only. This confirms that

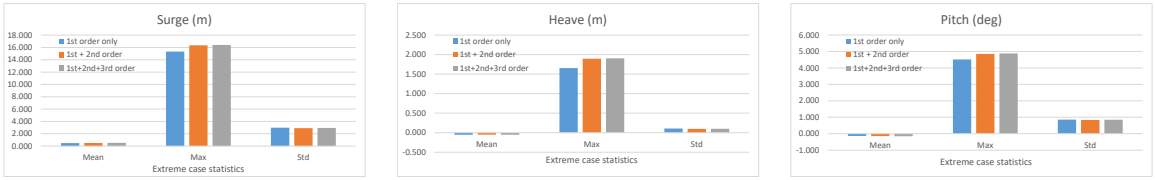

Fig. 15 Platform Surge, Heave, and Pitch Statistics, Extreme Case

Table 6 FOWT Response Statistics for Extreme Case

	1st order only			1st + 2nd order			1st+2nd+3rd order		
	Mean	**Max**	**Std**	**Mean**	**Max**	**Std**	**Mean**	**Max**	**Std**
Wave elevation (m)	0.001	12.732	3.169	0.001	12.732	3.169	0.001	12.732	3.169
Surge (m)	0.482	15.326	2.979	0.505	16.347	2.900	0.522	16.402	2.947
Heave (m)	-0.054	1.656	0.106	-0.050	1.895	0.097	-0.052	1.906	0.101
Pitch (deg)	-0.141	4.517	0.857	-0.148	4.852	0.834	-0.152	4.881	0.848
Tower BMy (kN.m)	-18689	332578	34324	-18833	298304	43537	-18961	331886	44812
L1 tension (kN)	4544.7	7062.8	449.0	4568.0	7481.6	507.8	4568.7	7518.7	506.6
L4 tension (kN)	4509.9	6536.0	340.8	4541.5	7026.8	388.8	4541.3	6996.2	389.1
L7 tension (kN)	4513.8	6783.2	374.4	4546.2	7223.2	421.6	4546.2	7209.8	421.7

the 3rd order wave load influence is much lower than those from the 2nd order wave loads. It is also observed that in the first order wave load only case the, maximum responses are not necessarily lower than those with 2nd and 3rd order wave loads. The maximum surge, pitch in the fatigue load case and the maximum tower base bending moment in the extreme load case are three examples in this study. However, only one random wave seed in each of the fatigue and extreme load cases is applied in the dynamic simulations. These observations can be considered as outliers and are not general conclusions. The evidence is that the standard deviation values in these three responses for the first order wave only cases are not higher than those cases with then 2nd and 3rd order wave loads.

10. Conclusions

The influence of the second and third order wave loads on the TLP FOWT responses are investigated in this study. The second order wave loads are calculated by commercial wave diffraction/radiation analysis software tool. The third order wave loads calculation methods are developed in this study based on the well-known FNV formulation. The third order wave force is applied on the platform in dynamic simulation models as external force. The following observations are made:

- The 2nd order wave loads have more influences on the FOWT responses than the 3rd order wave loads in both fatigue and extreme load cases. The 3rd order wave force influence is negligible in fatigue load cases, and more significant in extreme load cases.
- The high order wave loads have more impact on the tower and mooring system responses than platform motion. On a TLP FOWT, the tower and mooring system usually feature

high frequency resonance susceptible to excitation from sum frequency 2nd and 3rd order wave loads.

- The second and third order wave forces have significant impact on the tower dynamic responses.

References

Abramowitz, M. and Stegun, I. (1964), "Handbook of mathematical functions with formulas, graphs, and mathematical tables".

Bachynski, E. and Moan, T. (2014), "Ringing loads on tension leg platform wind turbines", *Ocean Eng*., **84**, 237-248. https://doi.org/10.1016/j.oceaneng.2014.04.007.

Bachynski, E.E. and Moan, T. (2012), "Design considerations for tension leg platform wind turbines", *Mar. Struct*., **29**(1), 89-114. https://doi.org/10.1016/j.marstruc.2012.09.001.

Bae, Y.H. and Kim, M.H. (2011), "Discussion on rotor-floater-mooring coupled dynamic analysis of mono-column-TLP-type FOWT (Floating Offshore Wind Turbine)", *Ocean Syst. Eng*., **1**(3), 243-248. https://doi.org/10.12989/ose.2011.1.3.243.

Bae, Y.H. and Kim, M.H. (2011), "Rotor-floater-mooring coupled dynamic analysis of mono-column-TLP-type FOWT (Floating Offshore Wind Turbine)", *Ocean Syst. Eng*., **1**(1), 95-111. https://doi.org/10.12989/ose.2011.1.1.095.

Bae, Y.H. and Kim, M.H. (2013), "Rotor-floater-tether coupled dynamics including 2nd-order sum-frequency wave loads for a mono-column-TLP-type FOWT (floating offshore wind turbine)", *Ocean Eng*., **61**, 109-122. https://doi.org/10.1016/j.oceaneng.2013.01.010.

Faltinsen, O.M., Newman, J.N. and Vinje, T. (1995), "Nonlinear wave loads on a slender vertical cylinder", *J. Fluid Mech*., **289**, 179-198. https://doi.org/10.1017/S0022112095001297.

Luke, Y.L. (1969), "The special functions and their approximations", **1**, Academic Press, Inc.

Malenica, S. and Molin B. (2006), "Third-harmonic wave diffraction by a vertical cylinder", *J. Fluid Mech*., **302**, Published online by Cambridge University Press.

Newman, J.N. (1996), "Waves and nonlinear processes in hydrodynamics. Kluwer, Ch. Nonlinear scattering of long waves by a vertical cylinder", 91-102.

Teng, B. and Dong, G. (2001), "Numerical examination of third-order wave force on axisymmetric bodies", *Int. J. Offshore Polar Eng*., **11**(4), ISOPE-01-11-4-248.

Tromans, P., Swan, C. and Masterton, S. (2006), "Nonlinear potential flow forcing: the ringing of concrete gravity based structures", Tech. Rep. Research Report 468, Health and Safety Executive.

MK